

PAPER • OPEN ACCESS

## Flip chip bonding on stretchable printed substrates; the effects of stretchable material and chip encapsulation

To cite this article: Muhammad Hassan Malik *et al* 2023 *Flex. Print. Electron.* **8** 015004

View the [article online](#) for updates and enhancements.

You may also like

- [Stretchable printed circuit board integrated with Ag-nanowire-based electrodes and organic transistors toward imperceptible electrophysiological sensing](#)  
Rei Kawabata, Tepei Araki, Mihoko Akiyama *et al.*
- [Printable stretchable interconnects](#)  
Wenting Dang, Vincenzo Vinciguerra, Leandro Lorenzelli *et al.*
- [Review—Flexible and Stretchable Electrochemical Sensing Systems: Materials, Energy Sources, and Integrations](#)  
Itthipon Jeerapan and Sujittra Poorahong

### ECS Toyota Young Investigator Fellowship



For young professionals and scholars pursuing research in batteries, fuel cells and hydrogen, and future sustainable technologies.

At least one \$50,000 fellowship is available annually.  
More than \$1.4 million awarded since 2015!



Application deadline: January 31, 2023

**Learn more. Apply today!**

# Flexible and Printed Electronics



## PAPER

# Flip chip bonding on stretchable printed substrates; the effects of stretchable material and chip encapsulation

### OPEN ACCESS

RECEIVED  
28 November 2022

REVISED  
9 January 2023


ACCEPTED FOR PUBLICATION  
13 January 2023

PUBLISHED  
24 January 2023

Original content from this work may be used under the terms of the [Creative Commons Attribution 4.0 licence](https://creativecommons.org/licenses/by/4.0/).

Any further distribution of this work must maintain attribution to the author(s) and the title of the work, journal citation and DOI.



Muhammad Hassan Malik<sup>1,2</sup>, Jaroslaw Kaczynski<sup>1</sup>, Hubert Zangl<sup>2,3</sup> and Ali Roshanghias<sup>1,\*</sup> 

<sup>1</sup> Silicon Austria Labs GmbH, Europastrasse 12, A-9524 Villach, Austria

<sup>2</sup> Institute for Smart Systems Technologies, Alpen-Adria-Universität Klagenfurt, 9020 Klagenfurt, Austria

<sup>3</sup> Silicon Austria Labs, AAU SAL USE Lab, Klagenfurt, Austria

\* Author to whom any correspondence should be addressed.

E-mail: [ali.roshanghias@silicon-austria.com](mailto:ali.roshanghias@silicon-austria.com)

**Keywords:** stretchable hybrid systems (SHS), ultra-thin chips (UTC), hybrid integration, printed electronics, anisotropic conductive paste (ACP), stretchable, Beyolex

## Abstract

Stretchable printed electronics have recently opened up new opportunities and applications, including soft robotics, electronic skins, human-machine interfaces, and healthcare monitoring. Stretchable hybrid systems (SHS) leverage the benefits of low-cost fabrication of printed electronics with high-performance silicon technologies. However, direct integration of silicon-based devices on conventional stretchable substrates such as thermoplastic polyurethane (TPU) and polydimethylsiloxane (PDMS) is extremely challenging due to their restricted low-temperature processing. In this study, a recently developed thermoset, stretchable substrate (Beyolex<sup>TM</sup>) with superior thermal and mechanical properties was employed to realize SHS via direct flip chip bonding. Here, ultra-thin chips (UTC) with a fine-pitch, daisy-chain structure was flip-chip bonded by using anisotropic conductive adhesives, while the complementary circuitry was facilitated via screen-printed, stretchable silver tracks. The bonded samples successfully passed reliability assessments after being subjected to cyclic 30% stretch tests for 200 cycles. The potential benefits of chip encapsulation after integration with the stretchable substrate to withstand larger strains were demonstrated by both mechanical simulation and experimental results.

## 1. Introduction

Stretchable electronic devices with high elastic mechanical responses are the key enablers of advanced technologies such as human-machine interfaces, soft robotics, and stretchable energy harvesting [1–5]. Also, the direct integration of electronics with biological tissues, such as human skin, with the goal of long-term health monitoring has been a highly sought-after topic [6]. On-skin electronics are expected to exhibit skin-like mechanical properties and sustain their electrical functions when exposed to a strain in the range of 30%. According to a previous study, the maximum strain the human skin can withstand is about 30% [7]. Several polymeric substrates with different rates of stretchability have so far been evaluated to build a stretchable circuit board. Thermoplastic polyurethane (TPU) has received the most attention, while polydimethylsiloxane (PDMS) and

polyurethane have also been used previously [8–15]. Likewise, several stretchable conducting materials, such as stretchable metallic inks, conducting polymers, carbon-based composites, and liquid metals, have been developed and successfully printed on those substrates [16–19].

Stretchable hybrid systems (SHS) are currently the mainstream for stretchable electronics since chip-less systems (similar to chip-less flexible) have not rendered high-performance and versatile products. The incorporation of rigid silicon-based components into a low-modulus stretchable substrate, on the other hand, may impact the overall system's stretchability and bendability. As a result, strain engineering in SHS systems is critical to impart total stretchability despite the existence of non-stretchable chips and interconnections. The goal of strain engineering is to minimize strain on rigid elements while localizing it on stretchable electrodes. Two approaches for SHS

have been pursued so far, namely embedding rigid or flexible islands in the stretchable parts as opposed to direct flipchip bonding on the stretchable. The embedding of the rigid island as a strain-relief structure or flexible printed circuit boards (PCB) containing several chips are the most common methodologies for SHS. Here, the interconnects to the stretchable electrodes are mostly fabricated after the embedding process, either via the built-up layers or on the surface. As an example, this approach has enabled several devices with enhanced performance, such as electrocardiogram devices, where all the chips were surface-mounted on a flexible PCB and then embedded in an elastomer. In that study, only the electrodes were exposed to high strain [20, 21]. Concerning the direct integration of rigid chips on the SHS, also known as the ‘chip-last approach’, few studies have been reported so far [22]. Here, the robust bonding of the chip pads to the stretchable substrates such as TPU or PDMS was rather challenging.

The first question for direct integration on a stretchable substrate is the interconnection approach, i.e. chip on board or flipchip bonding. Wire-bonding and conventional reflow soldering cannot be used on TPU because it has a low melting point (between 100 and 120 °C [23]) and a high coefficient of thermal expansion (220–473 ppm K<sup>-1</sup> [24]). Also, TPU is a soft material. Low-temperature solders were likely to work for flipchip bonding on Cu-plated TPU substrates, whereas conductive adhesives may be employed for high-pitch flipchip bonding on Ag-printed TPU. The options for fine-pitch flipchip bonding on TPU are non-conductive adhesives (NCA) and anisotropic conductive adhesive (ACA) bonding, which typically necessitate a higher processing temperature (>150 °C) [25]. In earlier work, Forester *et al* used TPU with copper-plated pads and bonded ultra-thin chips (UTC) by using NCA [24]. Bonding at 170 °C resulted in the melting and viscous flow of TPU, which served as an NCA covering the chip’s Au bumps. The common issues with NCA bonding, such as open circuits caused by the warpage of the substrate and height deviations on the chip, make ACA the preferred material. In a recent study, Behfar *et al* examined several ACA materials for bonding on TPU substrates and found that the ACA with a higher Young’s modulus could resist higher cycles of stretching [26]. They managed to ACA-bond TPU by heating the substrate and chip to 60 °C and 210 °C, respectively. Overall, the main obstacle to flipchip bonding on TPU is the low processing temperatures, which either limits the choice of ACA or hinders the ACA from curing properly at the desired temperatures. Consequently, the SHS success rate on TPU is relatively low. In this work, a recently-developed stretchable substrate with exceptional thermal stability is employed for ACA bonding. Based on our previous work on UTC directly integrated on printed flexible

substrates (paper and PET) using ACA [27, 28], we deploy an analogous ACA bonding strategy to realize SHS. As thinner dies could stand higher bending cycles on the other substrates and due to the substrate’s thermal stability, the robustness of the SHS gets improved.

## 2. Method

Figure 1(a) shows a demonstration of the test vehicle. The complementary daisy chain layouts on the stretchable substrate and the UTC are depicted in figures 1(b) and (c), respectively. UTCs with a thickness of 30 μm and a die size of 9 × 8 mm were utilized in this study. The thin chips were fabricated from an 8-inch silicon wafer using the Stealth Dicing Before Grinding process [27]. According to our previous studies, 30 μm UTC had a trade-off between die flexibility and handling yield during microassembly in the thickness range of 10–50 μm [27]. The chips were structured with eight parallel lines with a length of 4 mm and a varying width of 150–300 μm. These structures were fabricated via Cr (10 nm)/Au (100 nm) sputtering. In this study, a recently-developed, thermoset and non-silicone polymer film (Beyolox™, Panasonic, Japan) was employed as the stretchable substrate. The Beyolox film had a thickness of 100 μm and was provided with a 75 μm PEN carrier film as reinforcement during printing and bonding. Compared to TPU, Beyolox is more temperature resistant and compatible with the reflow assembly process. It can be stretched up to 200% and its thermal decomposition temperature is around 300 °C. The complementary daisy chain structures were screen printed on Beyolox using a stretchable Ag paste (LS453-6B, Asahi Kagaku, Japan) and then cured at 80 °C for 30 min.

The flipchip bonding process was conducted using a semi-automatic die bonder (Fineplacer lambda, Finetech GmbH). The UTC was picked up from the dicing tape and optically aligned with the substrate structure. Subsequently, an ACA (AC268, Delo, Germany) was dispensed in the designated area. The thermo-compression flipchip bonding was executed at 30 N bonding force for 10 sec, while the heating stage (substrate) and the tool (chip) were heated to ≥100 °C and ≥150 °C, respectively. An example of the ACA bonded UTC to the Beyolox is presented in figure 1(d).

The bonded area was later on protected using either the dry film lamination or glob top dispensing. In the case of lamination, a 25 μm polyimide film with a NCA film as an intermediate layer was laminated using hot lamination at 60 °C. In the case of Glob-top, a single component UV curable epoxy adhesive (OG116-31, Epotec, USA) was dispensed, and cured by both UV exposure and heating to 70 °C. The optical images of the test samples with both encapsulations are shown in figures 1(e) and (f).

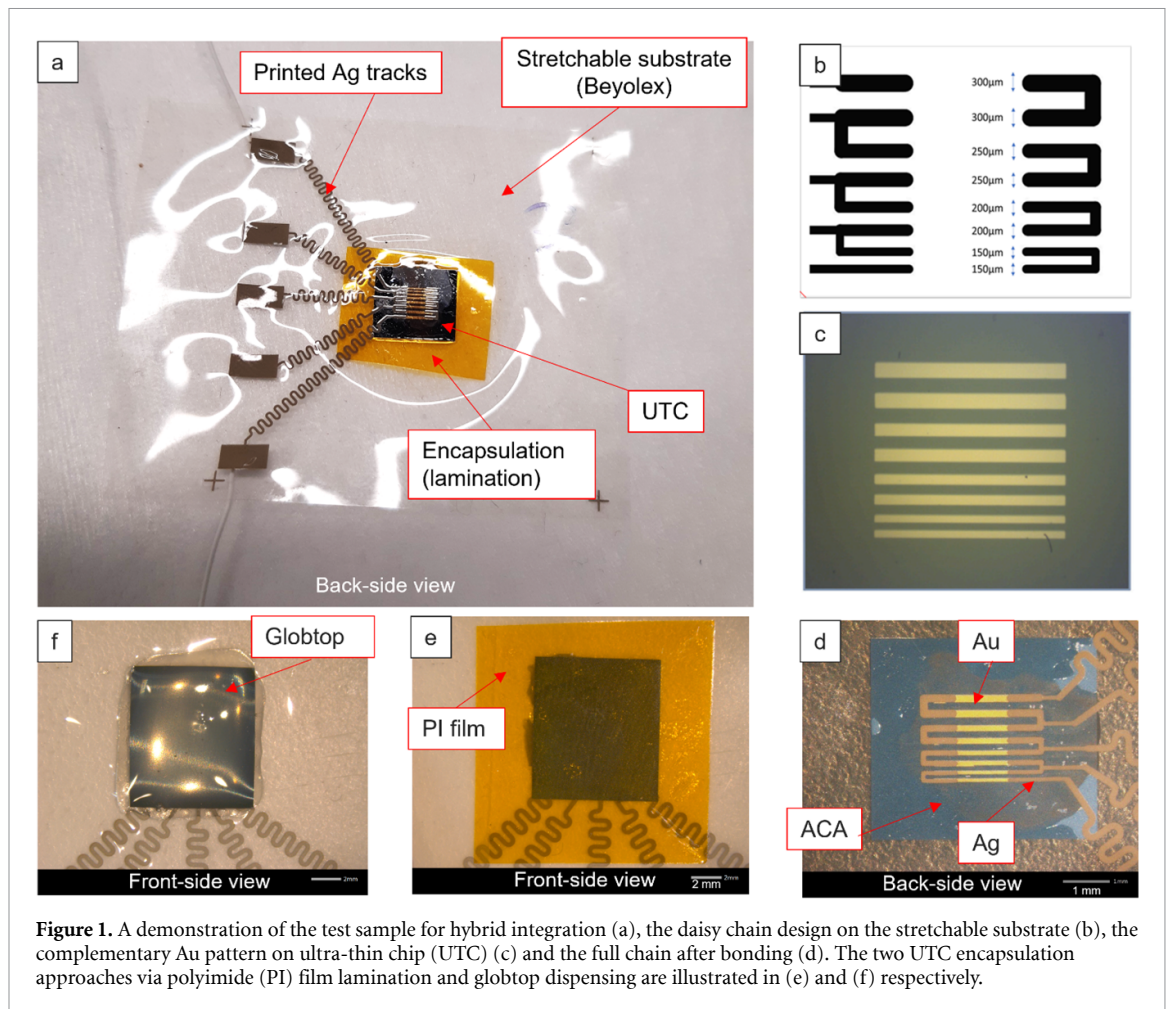


**Figure 1.** A demonstration of the test sample for hybrid integration (a), the daisy chain design on the stretchable substrate (b), the complementary Au pattern on ultra-thin chip (UTC) (c) and the full chain after bonding (d). The two UTC encapsulation approaches via polyimide (PI) film lamination and globtop dispensing are illustrated in (e) and (f) respectively.

A uniaxial tensile tester (ZwickRoell, Germany) was used to stretch five samples of each kind up to 30%. The daisy chains were electrically measured *in situ* using a two-point multimeter and external wires during both single-pull and cyclic loading testing. In order to understand the stress level and its distribution during the stretch test, finite element simulations using ANSYS 21.2 was also performed. Here, a model consisting of the Beyolex substrate with a size of  $40 \times 55$  mm, UTC, and PI lamination was built. The simulation was done at 30% strain.

### 3. Results and discussion

#### 3.1. Stretchability before chip mounting

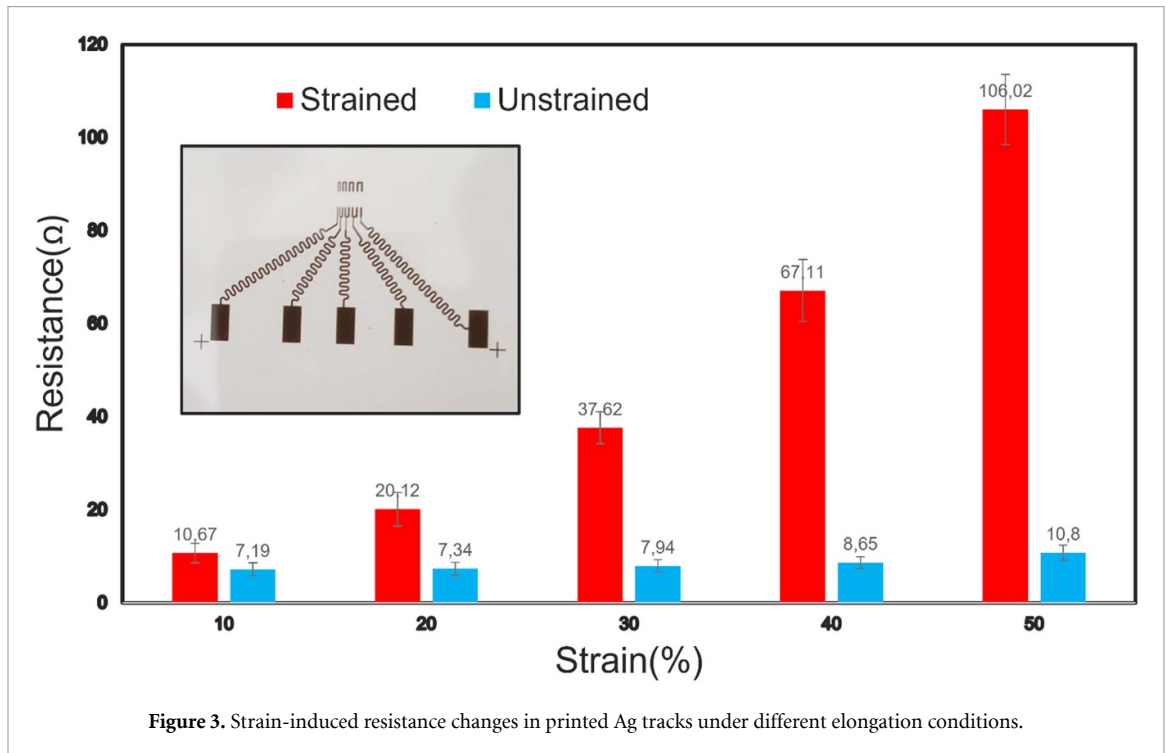
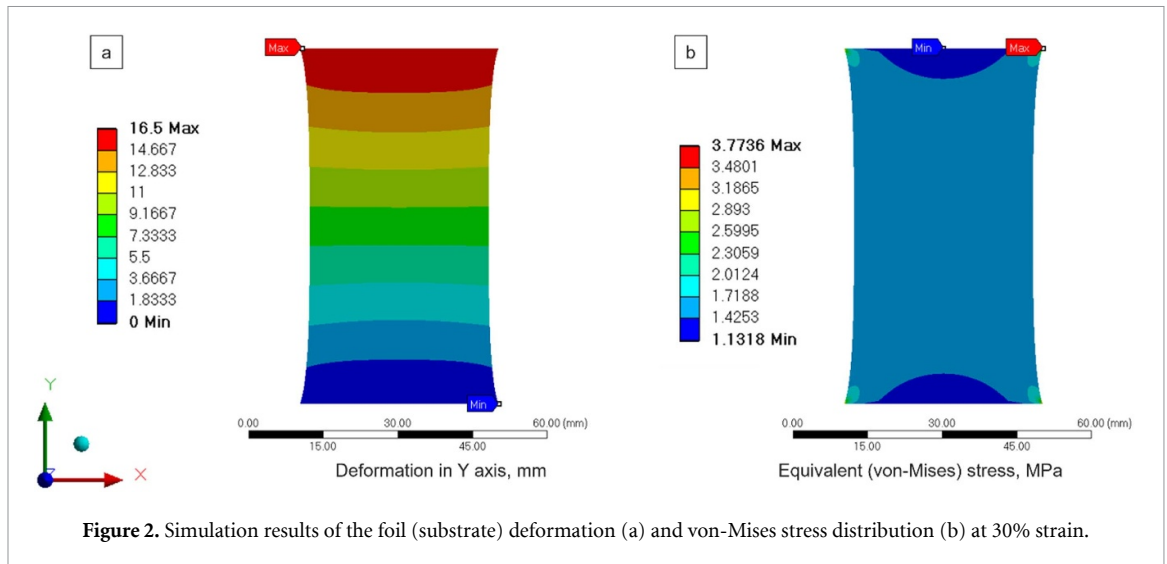
Beyolex is a fully stretchable substrate that can endure 200% elongation. However, as was previously mentioned, the target strain for the entire system in this study was set at 30%. The simulation results of the Beyolex foil deformation at 30% strain revealed that the width of the foil at its narrowest point (center-line of the foil) is reduced to 35.96 mm, i.e. 4.04 mm shorter than the original value and its length increases up to 16.5 mm (figure 2(a)). The maximum stresses evolved upon 30% elongation was around 3.7 MPa at the corners of the foil as shown in figure 2(b). These stresses were much lower than Beyolex's tensile

strength of 16 MPa. With the exception of the corners and edges, the von-mises stresses were almost constant at around 1.67 MPa.

Figure 3 depicts the strain-induced resistance variations of the printed Ag tracks up to 50%. The main objective of this analysis was to understand how printed lines behaved throughout the stretch test and prior to chip mounting. As seen in figures (1 and 3), the screen-printed Ag tracks had a serpentine structure. Also, based on the profilometry analysis, the Ag track possessed a thickness of  $10.2 \mu\text{m}$ . The unstrained, printed Ag tracks on Beyolex substrate had a sheet resistance of  $89 \pm 7 \text{ m}\Omega/\text{sq}$ . According to figure 3, the printed structures can sustain elongations of up to 50%. Figure 3 also implies that the resistance change is proportional to the percentage of strain. After strain release and a time-dependent recovery, the electrical conductivity of the printed tracks restores to near-original values. The unstrained results at larger strains, however, suggest that the conductivity of the Ag tracks marginally declined.

#### 3.2. Stretchability after chip mounting without encapsulation

During the flipchip bonding process, no discernible changes in the optical and mechanical characteristics of the Beyolex were observed. The UTC integration



on the Beyolex was conducted successfully without any noticeable electrical or mechanical failure. The DC resistance of the full daisy chain was around  $80 \pm 3 \Omega$  for all the bonded samples. It is worth noting that the identical flipchip bonding procedure on TPU failed owing to warpage and plastic deformation of TPU at the bonding temperature.

For the first stretchability assessments, the integrated UTC on Beyolex was examined by a single-pull test without any support or encapsulations. As shown in figure 4(a), the samples could withstand up to 20% elongation at the single-pull test and beyond that open circuits and loose contacts were detected. Additionally, UTC cracking was detected in some samples as shown in figure 4(b). The simulation results for these samples are presented in figure 5. Concerning

the foil deformation with the chip in the  $x$  and  $y$  direction, there were slight variations to the case without the chip (figure 5(a)). The highest elongation in the  $x$  direction (stretched direction) was +16.5, whilst a wavy-like pattern was detected in the  $y$  direction. The region along the chip contracted the least (3.8 mm), whereas the regions on the top and bottom sides of the foils (without the chip) contracted the most (4.1 mm).

The significant difference from the simulation without the chip was the 0.5 mm deformation of the film in the  $Z$  axis at the chip edges (figure 5(b)). Concerning the evolved stresses at 30% strain, the maximum stresses in the foil were at the corners of the chip which was about 4.6 MPa as illustrated in figure 5(c). The stresses in the chip itself were already

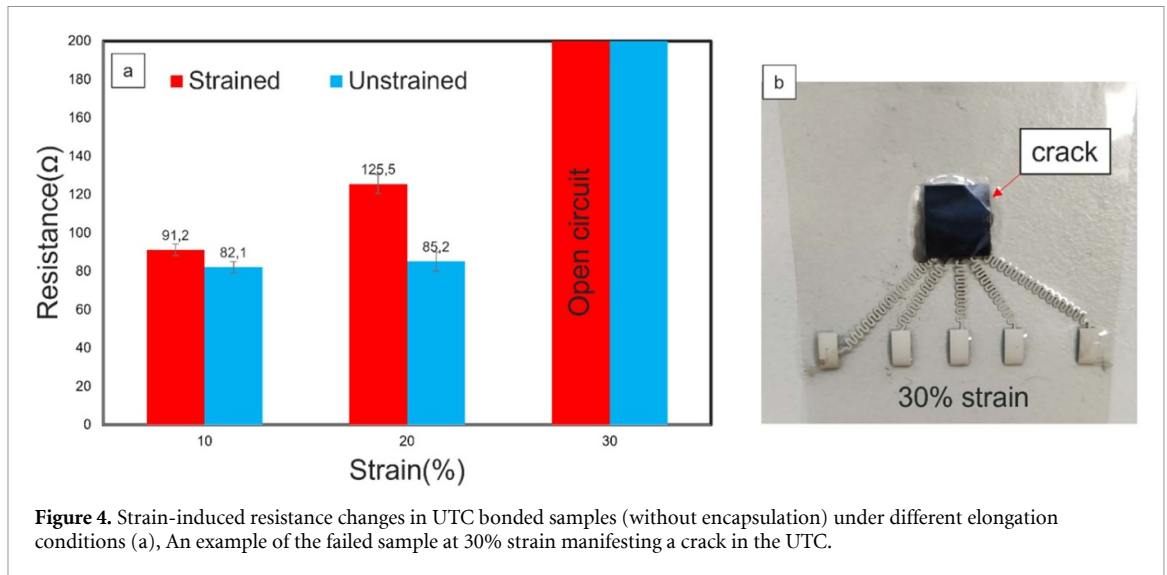


**Figure 4.** Strain-induced resistance changes in UTC bonded samples (without encapsulation) under different elongation conditions (a), An example of the failed sample at 30% strain manifesting a crack in the UTC.

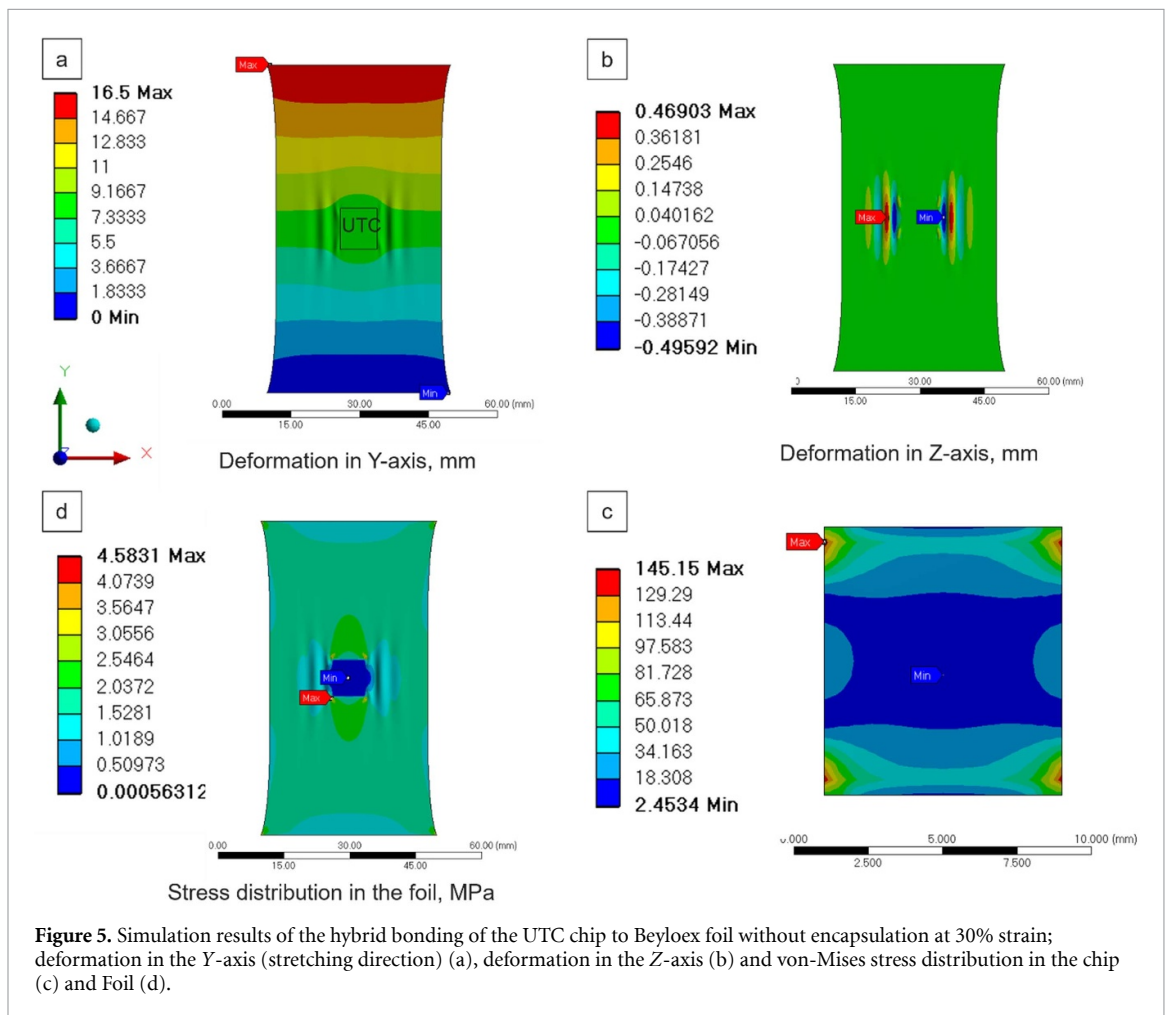


**Figure 5.** Simulation results of the hybrid bonding of the UTC chip to Beyloex foil without encapsulation at 30% strain; deformation in the Y-axis (stretching direction) (a), deformation in the Z-axis (b) and von-Mises stress distribution in the chip (c) and Foil (d).

much higher, reaching 145 MPa. UTC lacks stretchability despite being flexible. Being flexible makes UTC a great choice when the sample is exposed to bending, folding or twisting. Nonetheless, UTC is susceptible to cracking under tensile stress [29]. As a result, the failure of these samples at 30% strain was attributed to the UTC cracking, which was also verified experimentally (figure 4(b)). As a result, it became

evident that the transmission of tensile strain to the chip should be decreased.

### 3.3. Stretchability of the encapsulated chips

Based on the previous section’s findings, it was proposed to encapsulate the bonded UTC using PI lamination or globtop dispensing and examine them with the single pull test. It was reported that the

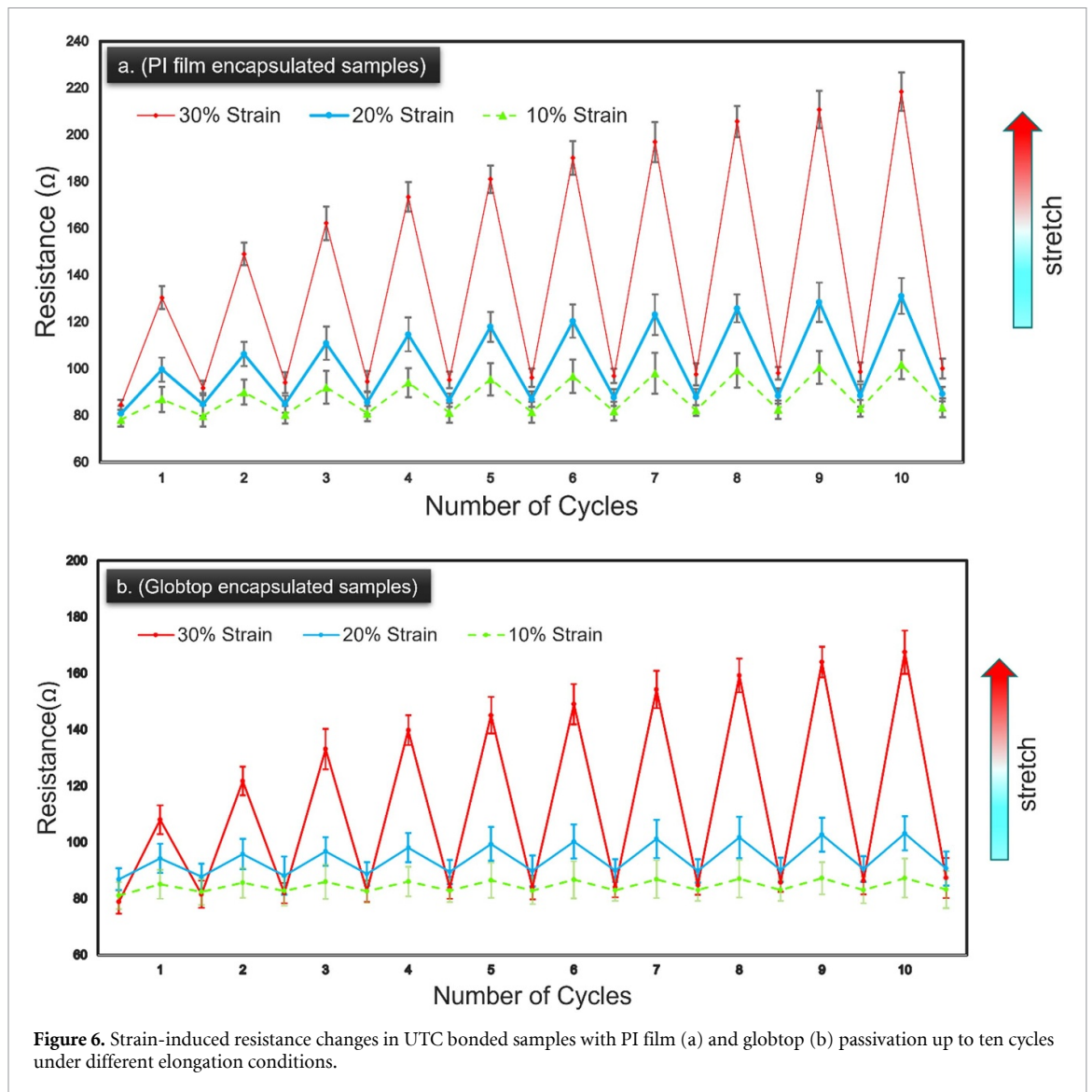


**Figure 6.** Strain-induced resistance changes in UTC bonded samples with PI film (a) and globtop (b) passivation up to ten cycles under different elongation conditions.

encapsulation of the chips increases the stiffness of the surrounding region, directing strain concentration from the chip corner to the foil [22, 30]. This time all the samples could pass the pull test at 30%. Subsequently, the samples were subjected to ten cycles of pull tests. Figure 6(a) shows the results of the stretch tests of the PI encapsulated UTCs for ten cycles at 10%, 20% and 30% strain. It was found that at 10% strain and after the ten cycles, the resistance increased from  $\sim 78 \Omega$  to  $\sim 101 \Omega$  and recovered back to  $\sim 83 \Omega$ . As for the 20% strain, the resistance increased from  $\sim 80 \Omega$  to  $\sim 131 \Omega$  after ten cycles and restored to  $\sim 88 \Omega$ . For 30% strain, the resistance increase was from  $\sim 84 \Omega$  to  $\sim 218 \Omega$  after ten cycles with a final recovery at  $100 \Omega$ . The same experiment was carried out for globe top encapsulated UTCs (figure 6(b)). Under 10% strain, the resistance increased from  $\sim 82 \Omega$  to  $\sim 87 \Omega$  after ten cycles with the final resistance being  $\sim 83 \Omega$ . For 20% and 30% strains, the change in resistance was  $\sim 86 \Omega$  till  $\sim 103 \Omega$  and  $\sim 72$  till  $167 \Omega$  respectively with  $\sim 90 \Omega$  and  $86 \Omega$  being the final resistance after recovery.

Conclusively, it was proved demonstrated that both types of encapsulated samples rendered enhanced performances which could withstand 30% strain in single-pull and cyclic tests. It is noteworthy to mention that all the samples could survive the ten cycles and no failures were recorded. The optical images of the encapsulated samples during the stretch tests are shown in figure 7.

Figure 8 depicts the simulation results of the encapsulated UTC. The  $y$ -direction deformation of the substrate revealed a more prominent wavy-like shape. The region along the encapsulated chip experienced the least  $y$ -axis deformation (3.52 mm), whereas the portions on the top and bottom sides of the foils (without the encapsulated chip) encountered the most contraction (4.18 mm). Identical stretch lines along the chip can be seen in both the simulation results shown in figures 8(a) and (b) and the optical image in figure 7. It was found that in an encapsulated chip the imposed stresses are more than three times lower than without passivation. Comparing figures 5(c) and 8(c) clearly shows that encapsulation

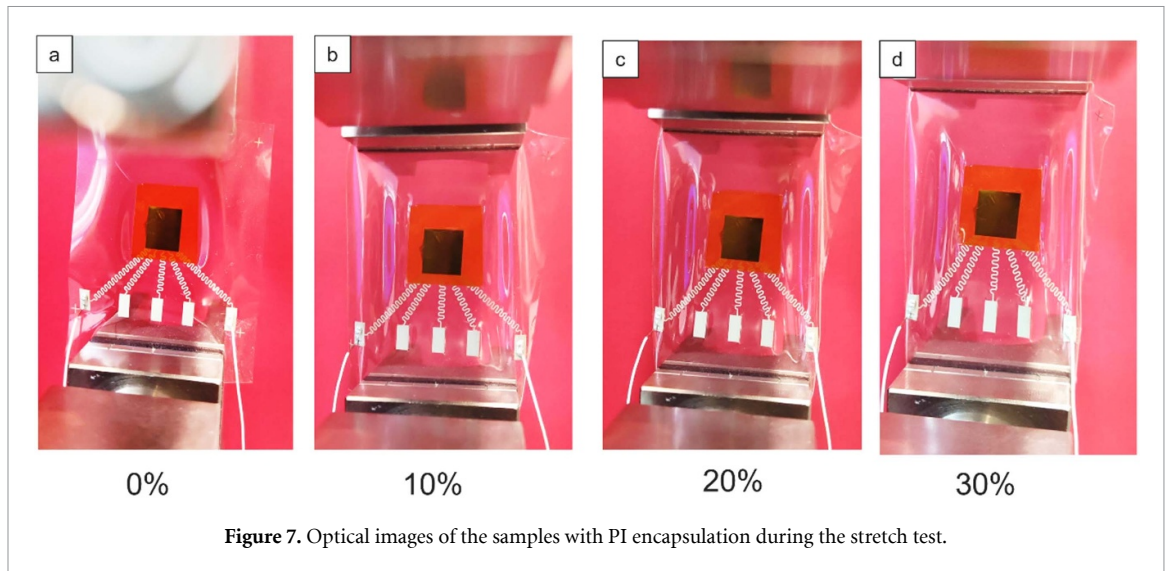


Figure 7. Optical images of the samples with PI encapsulation during the stretch test.

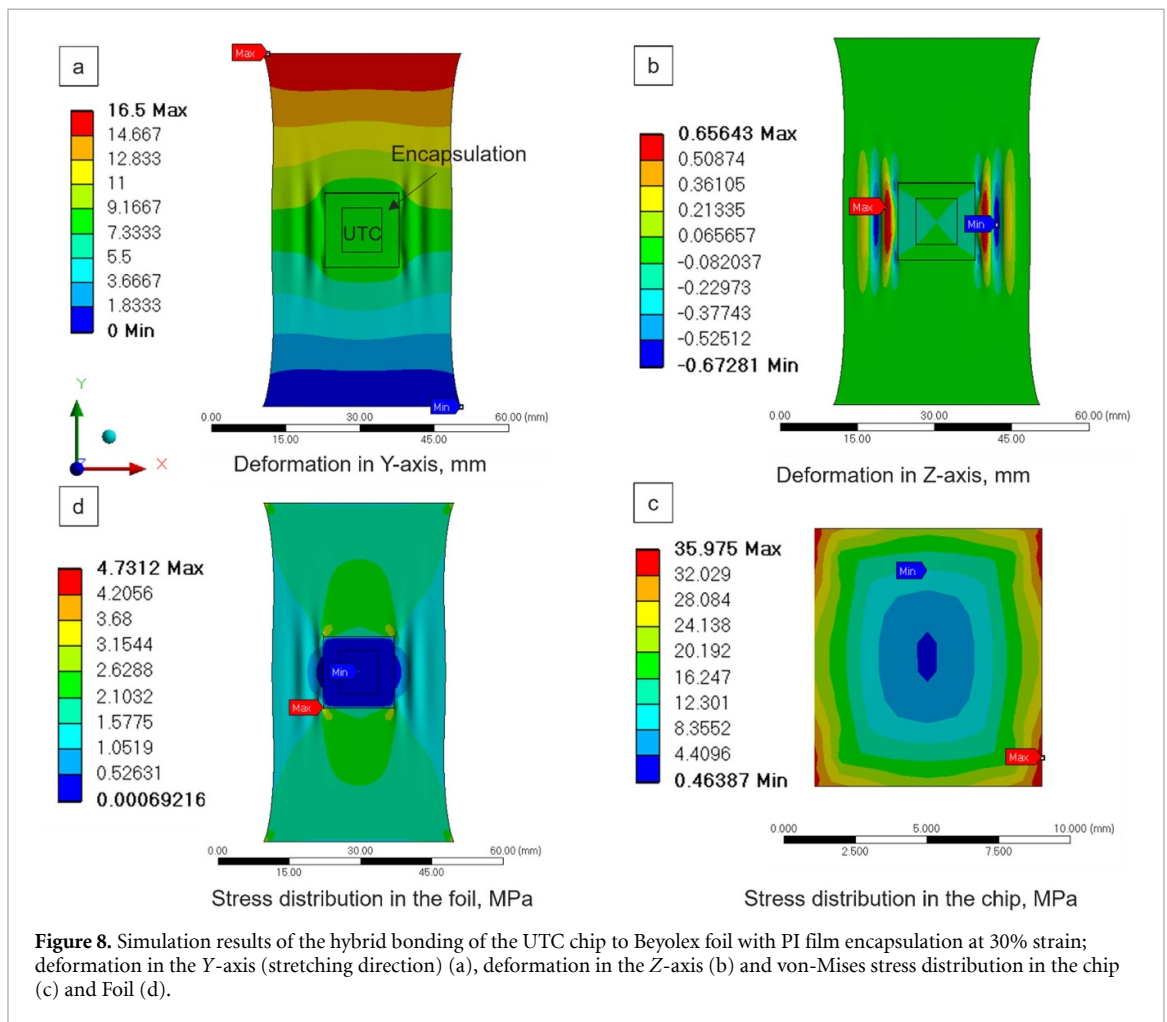


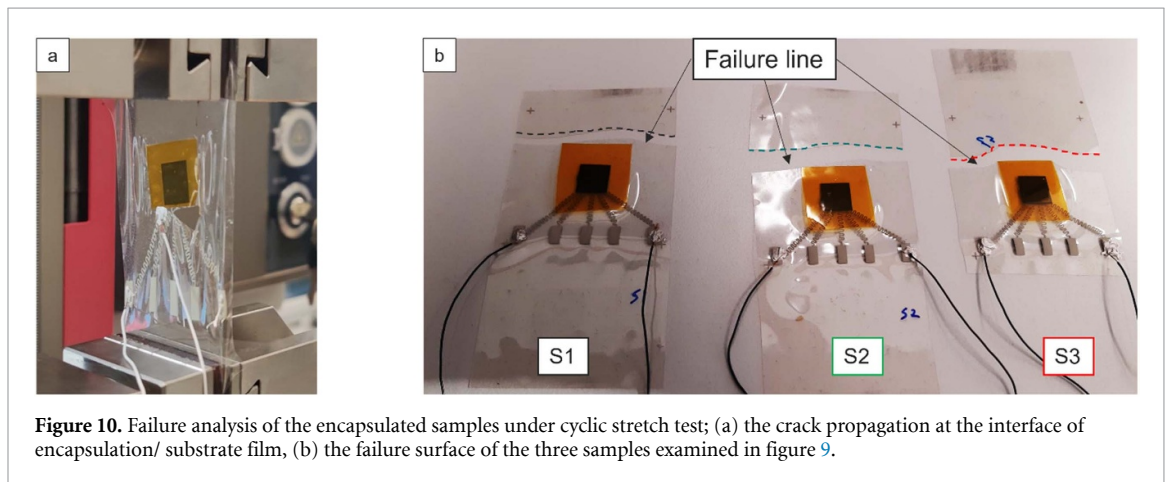
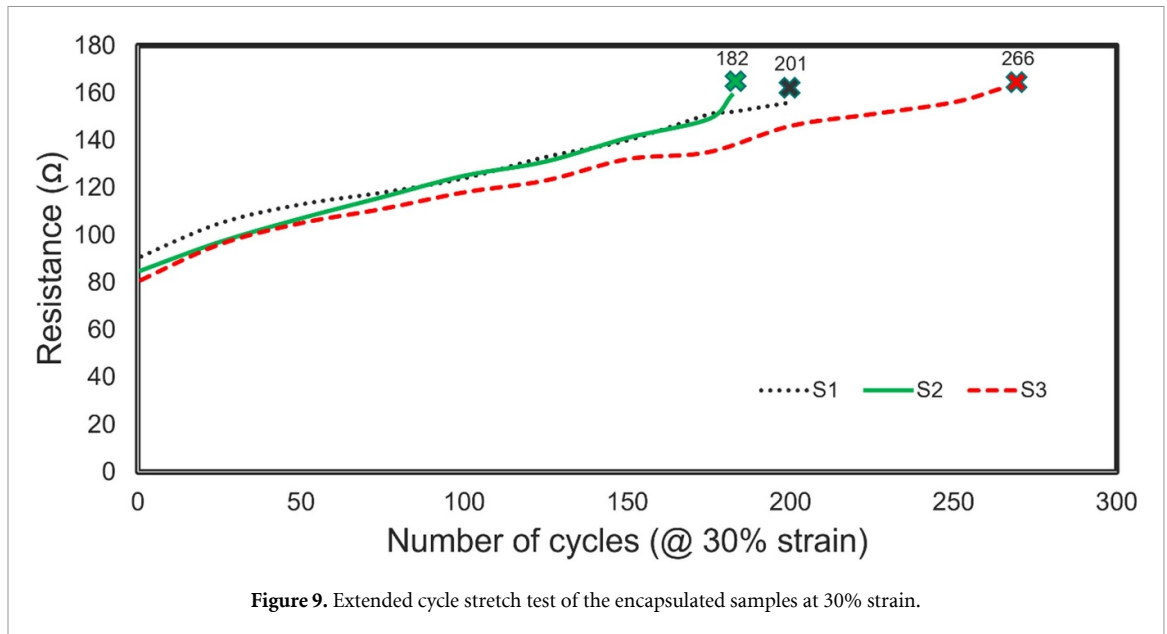
Figure 8. Simulation results of the hybrid bonding of the UTC chip to Beyolux foil with PI film encapsulation at 30% strain; deformation in the Y-axis (stretching direction) (a), deformation in the Z-axis (b) and von-Mises stress distribution in the chip (c) and Foil (d).

reduces the maximum tensile stress on the UTC from 145 MPa to 36 MPa.

Moreover, the results implied that the encapsulation further distributes the stresses in the transition between the chip and the substrate over a larger area. Notably, the employed ACA also featured a high Young's modulus (3.9 GPa) to secure the chip-to-substrate connections. A previous study that

assessed the stretchability of various ACA types discovered that those with higher Young's moduli can efficiently withstand the mechanical load exerted on the chip/substrate contact during cyclic strain [26]. Robust interconnects for SHS are therefore achievable with high modulus ACA. In a similar way, the encapsulation created a stiffer zone, resulting in reduced strain at a sensitive area under the same load.





### 3.4. Reliability analysis

After assessing the results in 3.3 and determining the top-performing samples, the long-term reliability of those samples was examined using an extended cycle stretch test at 30% strain. The goal was to determine the failure cycle and its location. Although both globtop and PI encapsulation produced similar results in prior experiments, PI encapsulation was favored for the reliability tests due to its superior uniformity, reproducibility and ease of processing. Figure 9 depicts the resistance-cycle curves of three samples. As can be observed, the samples failed in a range of 182–266 cycles. The failures, however, were not related to the electrical connections or the daisy chain, but to the substrate foil itself. Figures 10(a) and (b) shows optical images of the fractured samples. Despite the fact that all of the samples were still electrically functioning, the stretch test had to be terminated because of a rupture at the substrate/encapsulation interface. Figure 10(a) also depicts the emergence of the cracking from the

PI corner and how it spread along the PI edge. Figure 10(b) implies that all the samples failed at the same interface. Looking at figure 8(d) again, it is evident that the stress concentration points are located in the corners of the encapsulation film. As a result, it can be deduced that the system's weak spots were shifted from the brittle UTC corner for non-encapsulated samples to a more ductile region (PI corners) for encapsulated ones. The encapsulated sample was able to tolerate 30% strain for around 200 cycles because of this stress mitigation and strain engineering.

### 4. Conclusion

In this study, direct flipchip bonding of UTC on a recently-developed stretchable substrate 'Beyolex' was explored to realize a SHS. Compared to TPU and PDMS, Beyolex offers higher process temperatures, therefore thermocompression ACA bonding succeeded without any deformation and degradation.

The results of the single-pull and cyclic stretch test revealed that the stretchability of UTC-bonded samples without encapsulation is limited to 20% due to early fracture at the UTC. On the other hand, the application of a thin polyimide film or a globtop layer on top of the chip significantly enhances the performance of the samples by reducing the imposed stresses on the chip area. The encapsulated samples could tolerate 30% strain for around 200 cycles. The failure analysis and simulation results indicate that the weak points after encapsulation shifted from the sensitive UTC area to the edges of the encapsulation film, which caused higher endurance during the stretch test. Conclusively, it can be deduced that direct fine-pitch flipchip bonding yield a reliable SHS incorporating UTC, high modulus ACA, stretchable substrate with enhanced thermal and mechanical properties, and chip encapsulation.

### Data availability statement

The data that support the findings of this study are available upon reasonable request from the authors.

### Acknowledgments

This work has received funding from the "European Regional Development Fund" (EFRE) and "REACT-EU" (as a reaction of the EU to the COVID-19 pandemic) by the Kaerntner Wirtschaftsfor-derungs Fonds" (KWF) within the project Pattern-Skin (16048/34262/49709). The authors gratefully acknowledge Mr. Tsuyoshi Takeda from Panasonic Industry Company for the material support

### Conflict of interest

The authors declare that they have no known competing financial interests or personal relationships that could have appeared to influence the work reported in this paper.

### Authorship contribution statement

**M H Malik:** Methodology, Formal Analysis, Investigation, Writing original draft. **J Kaczynski:** Software, Writing—review & editing. **H Zangl:** Supervision, Writing—review & editing, Funding acquisition. **A Roshanghias:** Conceptualization, Methodology, Visualization, Writing original draft, Supervision, Project administration.

### Ethics statement

This article does not contain any studies involving human or animal participants.

### ORCID iD

Ali Roshanghias  <https://orcid.org/0000-0002-0463-3337>

### References

- [1] Trung T Q and Lee N-E 2017 Recent progress on stretchable electronic devices with intrinsically stretchable components *Adv. Mater.* **29** 1603167
- [2] Lim S et al 2015 Transparent and stretchable interactive human machine interface based on patterned graphene heterostructures *Adv. Funct. Mater.* **25** 375–83
- [3] Gonzalez M, Axisa F, Bulcke M V, Brosteaux D, Vandeveldel B and Vanfleteren J 2008 Design of metal interconnects for stretchable electronic circuits *Microelectron. Reliab.* **48** 825–32
- [4] Huang X et al 2014 Materials and designs for wireless epidermal sensors of hydration and strain *Adv. Funct. Mater.* **24** 3846–54
- [5] Roh E, Hwang B-U, Doil K, Bo-Yeong K and Lee N-E 2015 Stretchable, transparent, ultrasensitive, and patchable strain sensor for human-machine interfaces comprising a nanohybrid of carbon nanotubes and conductive elastomers *ACS Nano* **9** 6252–61
- [6] Fan J, Yeo W H and Su Y 2014 Fractal design concepts for stretchable electronics *Nat. Commun.* **5** 1–8
- [7] Gallagher A J, Annaidh A N and Karine B 2012 Dynamic tensile properties of human skin *IRCOBI Conf. 2012 (Dublin (Ireland), 12–14 September 2012)* (International Research Council on the Biomechanics of Injury) (<https://doi.org/10.1111/j.1095-8649.2012.03235.x>)
- [8] Wang S, Nie Y, Zhu H, Yurui X, Cao S, Zhang J, Yanyan L, Wang J, Ning X and Kong D 2022 Intrinsically stretchable electronics with ultrahigh deformability to monitor dynamically moving organs *Sci. Adv.* **8** eabl5511
- [9] Lee B, Cho H, Jeong S, Yoon J, Jang D, Lee D K, Kim D, Chung S and Hong Y 2022 Stretchable hybrid electronics: combining rigid electronic devices with stretchable interconnects into high-performance on-skin electronics *J. Inf. Disp.* **23** 163–84
- [10] Wei W 2019 Stretchable electronics: functional materials, fabrication strategies and applications *Sci. Technol. Adv. Mater.* **20** 187–224
- [11] Sun J-Y, Lu N, Yoon J, Oh K-H, Suo Z and Vlassak J J 2009 Inorganic islands on a highly stretchable polyimide substrate *J. Mater. Res.* **24** 3338–42
- [12] Pramoda K P, Chung T S, Liu S L, Oikawa H and Yamaguchi A 2000 Characterization and thermal degradation of polyimide and polyamide liquid crystalline polymers *Polym. Degrad. Stab.* **67** 365–74
- [13] Miranda C, Castaño J, Valdebenito-Rolack E, Sanhueza F, Toro R, Bello-Toledo H, Uarac P and Saez L 2020 Copper-polyurethane composite materials: particle size effect on the physical-chemical and antibacterial properties *Polymers* **12** 1934
- [14] Khan A, Roo J S, Kraus T and Steimle J 2019 Soft inkjet circuits: rapid multi-material fabrication of soft circuits using a commodity inkjet printer *Proc. 32nd Annual ACM Symp. on User Interface Software and Technology (New Orleans, LA, USA)*
- [15] Jahanshahi A, Gonzalez M, Jeroen V D B, Bossuyt F, Vervust T, Verplancke R, Vanfleteren J and Johan D B 2013 Stretchable circuits with horseshoe shaped conductors embedded in elastic polymers *Jpn. J. Appl. Phys.* **52** 05DA18
- [16] Freire M T D A, Damant A P, Castle L and Reyes F G R 1999 Thermal stability of polyethylene terephthalate (PET): oligomer distribution and formation of volatiles *Packag. Technol. Sci.* **12** 29–36
- [17] Liu S-H, Shen M-Y, Kuan C-F, Kuan H-C, Ke C-Y and Chiang C-L 2019 Improving thermal stability of

- polyurethane through the addition of hyperbranched polysiloxane *Polymers* **11** 697
- [18] Kim D H, Ahn J H, Choi W M, Kim H S, Kim T H, Song J, Huang Y Y, Liu Z, Lu C and Rogers J A 2008 Stretchable and foldable silicon integrated circuits *Science* **320** 507–11
- [19] Zhu G-J, Ren P-G, Guo H, Jin Y-L, Yan D-X and Li Z-M 2019 Highly sensitive and stretchable polyurethane fiber strain sensors with embedded silver nanowires *ACS Appl. Mater. Interfaces* **11** 23649–58
- [20] Kim Y-S, Mahmood M, Lee Y, Kim N K, Kwon S, Herbert R, Kim D, Cho H C and Yeo W-H 2019 All-in-one, wireless, stretchable hybrid electronics for smart, connected, and ambulatory physiological monitoring *Adv. Sci.* **6** 503–12
- [21] Fernandes D, Majidi C and Tavakoli M 2019 Digitally printed stretchable electronics: a review *J. Mater. Chem. C* **7** 14035–68
- [22] Gillan L, Hiltunen J, Behfar M H and Rönkä K 2022 Advances in design and manufacture of stretchable electronics *Jpn. J. Appl. Phys.* **61** SE0804
- [23] matweb (available at: [www.matweb.com/search/datasheet.aspx?matguid=9f5318a1f93b403bbd5748abec70fac1&ckck=1](http://www.matweb.com/search/datasheet.aspx?matguid=9f5318a1f93b403bbd5748abec70fac1&ckck=1)) (Accessed 02 November 2022)
- [24] Foerster P, Dils C, Kallmayer C, Löher T and Lang K D, 2012 First approach to cost-efficient fine pitch NCA flip-chip assembly on thermoplastic polyurethane printed circuit boards *2012 4th Electronic System-Integration Technology Conf. (September 2012)* (IEEE) pp 1–6
- [25] Delo-adhesives (available at: [www.delo-adhesives.com/service-center/downloads/downloads/datasheet/DELO%20MONOPOX\\_AC268\\_TIDB-en.pdf?show=1&type=5001&cHash=39489453a92d624c4dafb22f7ea499a5](http://www.delo-adhesives.com/service-center/downloads/downloads/datasheet/DELO%20MONOPOX_AC268_TIDB-en.pdf?show=1&type=5001&cHash=39489453a92d624c4dafb22f7ea499a5)). (Accessed 2 November 2022)
- [26] Behfar M H, Khorramdel B, Korhonen A, Jansson E, Leinonen A, Tuomikoski M and Mäntysalo M 2021 Failure mechanisms in flip-chip bonding on stretchable printed electronics *Adv. Eng. Mater.* **23** 2100264
- [27] Malik M H, Grosso G, Zangl H, Binder A and Roshanghias A 2021 Flip chip integration of ultra-thinned dies in low-cost flexible printed electronics; the effects of die thickness, encapsulation and conductive adhesives *Microelectron. Reliab.* **123** 114204
- [28] Malik M H, Rauter L, Zangl H, Binder A and Roshanghias A, 2022 Ultra-thin chips (UTC) integration on inkjet-printed papers *2022 IEEE Int. Conf. on Flexible and Printable Sensors and Systems (FLEPS) (Vienna)*
- [29] Takeshita T, Takei Y and Yamashita T 2020 Atsushi Oouchi and Takeshi Kobayashi, “flexible substrate with floating island structure for mounting ultra-thin silicon chips,” *Flex. Print. Electron.* **5** 025001
- [30] Behfar M H, Di Vito D, Korhonen A, Nguyen D, Amin B M, Kurkela T, Tuomikoski M and Mäntysalo M 2021 Fully integrated wireless elastic wearable systems for health monitoring applications *IEEE Trans. Compon. Packag. Manuf. Technol.* **11** 1022–7